IEEE *Access*

Analysis of a Real-Time FSO System Utilizing Xia and SRRC Pulses in Multi-band Carrier-Less Amplitude and Phase Modulation

Paul Anthony Haigh[1], Mojtaba Mansour Abadi[2], Zabih Ghassemlooy[2], Nguyen The Quang[3], Son Thai Le[4] and Nguyen Tan Hung[5]

[1]Newcastle University, School of Engineering, United Kingdom.
[2]Optical Communications Research Group, Northumbria University, United Kingdom
[3]Le Quy Don Technical University, Hanoi, Viet Nam
[4]Nokia Bell Labs, Holmdel, New Jersey, USA
[5]The Advanced Institute of Science and Technology, University of Danang, Viet Nam.
Corresponding author: Nguyen Tan Hung (e-mail: hung.nguyen@ac.udn.vn).

ABSTRACT In this paper, we investigate the impact of two pulse shapes on the performance of a real-time free-space optical communication link. The two candidate pulse shapes are the square-root raised cosine and Xia pulse, respectively which are tested as the basis function for multi-band carrier-less amplitude and phase modulation. We first develop a real-time system based on a Xilinx Zynq ZCU102 system-on-chip platform utilising a high-resolution analogue-to-digital-converter. We then generate multi-band carrier-less amplitude and phase modulation formats using it and test the error vector magnitude whilst varying parameters. We emulate the fog environment utilising neutral density filters and evaluate the error performance of the link under increasingly poor visibility conditions. We show that contrary to previous reports, the SRRC pulse shape offers superior performance over the first-order Xia pulse in the FSO environment operating at data rates exceeding 1 Gb/s.

INDEX TERMS Advanced modulation formats, Carrier-less Amplitude and Phase Modulation, Communication Systems, Field-programmable gate arrays, Free-space optics

I. INTRODUCTION

Real-time free-space optical (FSO) systems are the focus of renewed research interest in recent years. FSO technology is increasingly being utilised to supply robust communication links in harsh environments such as inner-city networks, connections to remote communities [1], and celestial networks [2]. FSO technologies are easily inter-operable with existing network infrastructure, can be quickly and cheaply deployed and upgraded whilst seamlessly operating over long periods of time (in all weather conditions), making it an interesting choice for future network deployments [3].

One of the key challenges in FSO systems is that of changing weather conditions causing link outages and impairments, resulting in a large number of reports in this area. Fog can cause reduced visibility [4], acting as a neutral density filter. Turbulence impacts the refractive index along the signal path, resulting in beam wandering at the receiver due to optical power deflection from the direction of propagation [5]. To address this challenge, significant research effort has been put into comparing modulation formats and digital signal processing (DSP) techniques to see how they compare. For instance, there have been reports of quadrature amplitude modulation (QAM) [6], orthogonal frequency division multiplexing (OFDM) [7], differential phase shift keying (DQPSK) [6] and sub-carrier intensity modulation [8]. More recently, the performance of carrier-less amplitude and phase modulation (CAP) modulation has been evaluated in an FSO link [9]. Each of them offers bespoke advantages and disadvantages, indicating that a system capable of switching between different modulation formats would be an advantage.

Unfortunately, most real-time links demonstrated have utilised small form-factor pluggable (SFP) devices operating at gigabit speeds but restricting links to NRZ or PAM4 modulation, inflexibly [10]. This is a substantial disadvantage because it means that adaptation to specific weather conditions is impossible.

In recent years, CAP (and its multi-band counterpart, *m-*

CAP) have also been the focus of a huge amount of research interest within the optical wireless community, with a high number of demonstrations performed on visible light communications links [11], [12]. CAP utilises a basis function (normally a square-root raised cosine (SRRC)) and a Hilbert pair to transmit information over the channel. Lately, there have recently been reports of systems where different pulse shapes have been tested as the basis function for the Hilbert pair.

One of the most interesting is the Xia pulse, which is valid for both Nyquist and root-Nyquist operation simultaneously [13]. The majority of the power in its side-lobes is retained in the pre-cursor, and the post-cursor side-lobe decays much faster than the SRRC. This is an interesting aspect as it will impact on system performance; recent literature has shown that using the Xia pulse as the basis function can yield performance gains over the SRRC in offline systems [14]. Therefore, in this paper, we compare the SRRC with the Xia pulse in a real-time FSO system. Our real-time system is not based on an SFP module. We utilise an FPGA and a high-performance digital-to-analogue and analogue-to-digital pair, allowing us to test analogue modulation in real-time. The proposed m-CAP FSO platform is evaluated using an indoor controlled atmospheric chamber that emulates the foggy conditions that would occur outdoors. We have investigated a simulated fog environment by utilising neutral density filters (NDFs), which is a valid approach and has been reported previously in the literature [15]–[20]. In contrast to previous approach that relied on fog machines, this approach allows us to ensure that the power received is consistent without relying on a network of external atmosphere monitors that need to be calibrated and customised on an ongoing basis. We refer to the received power in our results rather than visibility, despite the fact that they are intrinsically interlinked, because there are several fog regimes that can be selected for a given received power,

so the particle size considered in each case would be different.

We demonstrate that our gigabit-class FSO system can support m-CAP modulation whilst utilising up to 20 sub-bands. We also demonstrate that for our system, the SRRC pulse offers superior performance to the Xia pulse in our m-CAP configuration.

The paper is organised as follows. The experimental test setup is described in Section II. The results are outlined and discussed in Section III, and finally, conclusions are drawn in section IV.

II. Experimental Test Setup

The schematic block diagram for the proposed experimental testbed is illustrated in Fig. 1. The FPGA platform used is a low-cost Xilinx Zynq ZCU102 system-on-chip (SoC), which features both an FPGA and a quad core ARM Cortex A53 processor. We note, however, that the system should be portable to other Xilinx UltraScale+ architectures with minor adjustment provided the replacement board has similar transceivers. In this system, we have built the data generator via Analog Devices industrial input-output library (LibIIO) and the respective Python bindings (PyADI-IIO). By using this package, we can generate and process pseudo-random data streams in a flexible way via the embedded Linux platform, ensuring compatibility with any variety of m-CAP without having to perform the time-consuming reprogramming of the FPGA. The SoC has two parts, the programmable logic (traditional FPGA) and the processing side. Data is passed between the two through direct memory access; the data stream is saved into shared memory on the processing side before being accessed by the programmable logic in the FPGA.

We are interested in analysing the performance of the FSO link using m-CAP modulation with different pulse shapes and in different atmospheric scenarios. The maximum
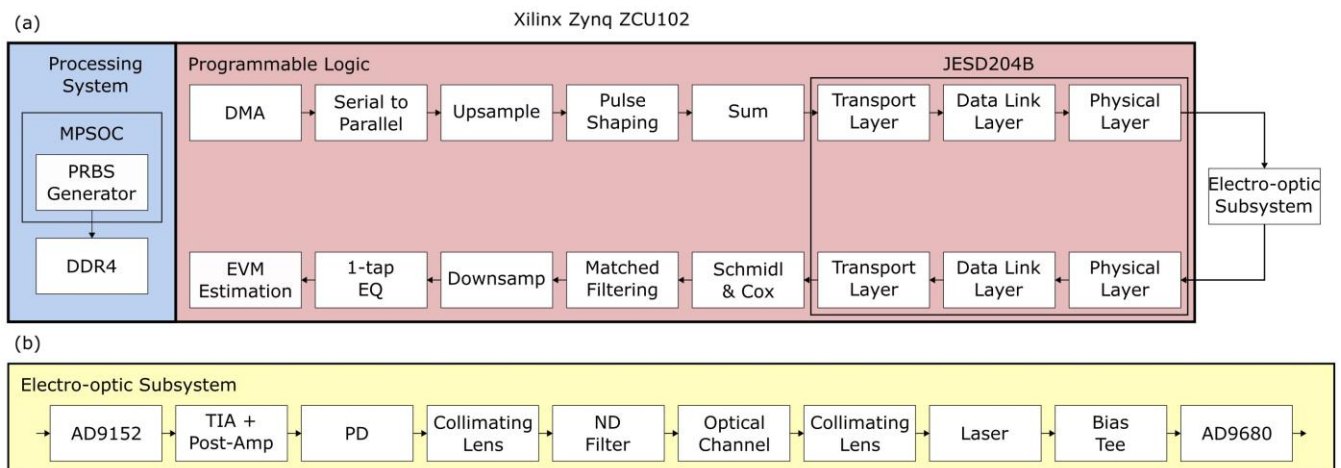

Fig. 1 The simplified block diagram of: (a) the system under test and the m-CAP modulation format. Abbreviations used: DDR4: double data rate 4, PRBS: pseudorandom binary sequence, DMA: direct memory access, AD: Analog Devices, PD: photodiode, TIA: transimpedance amplifier, ND: neutral density, EVM: error vector magnitude, EQ: equalisation, and (b) the electro-optic subsystem.

bandwidth available in the link was ~300 MHz and we vary our data rate via the modulation cardinality. We select $k = 2$, 4 and 6 bits/symbol. Alternatively, we could have selected an oversampling rate of 2, causing the useful bandwidth to double. During our initial tests, however, we found that the analogue bandwidth of the electro-optic components in the proposed system was better suited to an oversample rate of 4, thus limiting us to 300 MHz. After the data is loaded, it is mapped onto the appropriate quadrature amplitude modulation (QAM) constellation. The symbols are then up-sampled and pulse shaped using one of the two candidate filters under test, as will be described below.

The first candidate basis function for the pulse shaping filter is the SRRC pulse, given by [14]:

$$g_s(t)$$

$$= \frac{2\beta \left[\cos\left(\frac{(1+\beta)\pi t}{T_s}\right) + \sin\left(\frac{(1-\beta)\pi t}{T_s}\right)\left[\frac{4\beta t}{T_s}\right]^{-1}\right]}{\pi\sqrt{T_s}\left[1 - \left(\frac{4\beta t}{T_s}\right)^2\right]} \quad (1)$$

where T_s is the symbol period, t is the instantaneous time sample and β is the filter roll-off factor. Similarly, the first-order Xia pulse is defined as [14]:

$$g_x(t) = \frac{\sin\left(\frac{\pi t}{T_s}\right)\cos\left(\frac{\pi t \beta}{T_s}\right)}{\left(\frac{\pi t}{T_s}\right)(2\beta t + T_s)} \quad (2)$$

The pulse shapes of (1) and (2) with $\beta = 0.35$ and 300 MHz bandwidth are illustrated in Fig. 2. The Xia pulse is an asymmetric pulse with its peak slightly before the sampling instance. The majority of the power in its side-lobes is retained in the pre-cursor, and the post-cursor side-lobe decays much faster than the SRRC, offering advantages that have been demonstrated in visible light communications systems [14] but never in FSO.
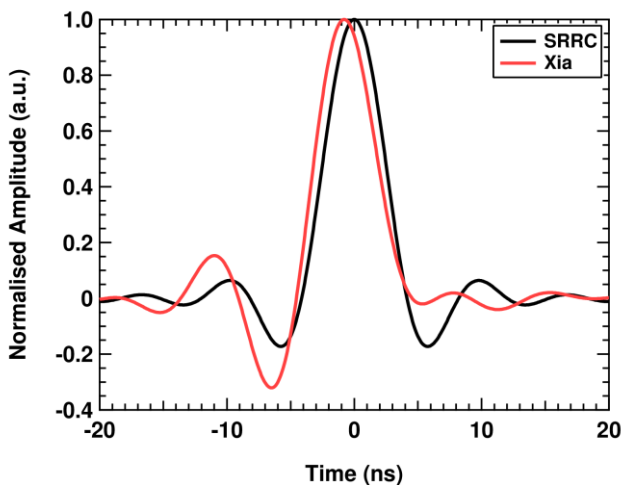

Fig. 2 The two pulse shapes under test with a roll-off factor of 0.35.

The excess energy factor β spreads the energy over the range of pulse shapes. Increasing values of β result in decreased sub-band transmission speeds following:

$$R_s = \frac{BW}{m(1 + \beta)} \quad (3)$$

Clearly, setting the value of β excessively will puncture the data rate, while setting it insufficiently will not provide a satisfactory guard band for the sub-bands. Therefore, we set this parameter to 0.1, 0.35, and 0.5 in order to test its impact on real-time links.

We set the value of m from the set $\{1, 5, 10, 20\}$, following up studies performed in visible light communications that showed improved error performance with an increasing number of sub-bands [21]. We the effect on varying m on the system bandwidth in Fig. 3. Clearly, splitting the bandwidth into increasingly smaller sub-bands approaches an OFDM-like solution where each sub-band has lower performance requirements. This combination of values results in baud rates ranging from 205-280 MBd for our link. Thus, when we select $k = 2$ (4-QAM), the system is effectively operating at ~0.5 Gb/s. Likewise, for $k = 4$ (16-QAM), the transmission rate is ~1 Gb/s, and for $k = 6$ (64-QAM), it is approximately 1.5 Gb/s.
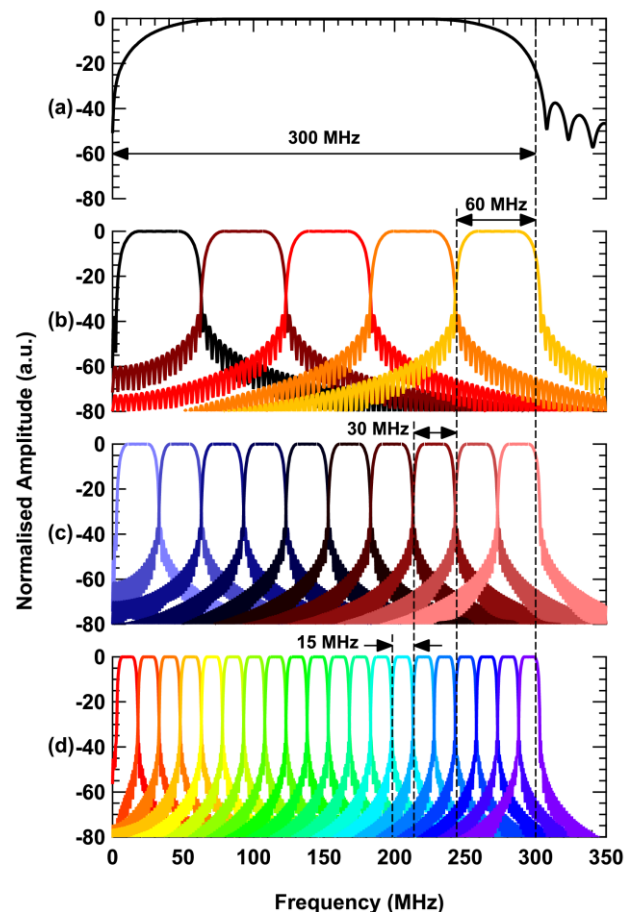

Fig. 3 Illustration of the concept of multi-band CAP: (a) 1-CAP, (b) 4-CAP, (c) 10-CAP and (d) 20-CAP. The same bandwidth is

divided into an increasing number of sub-bands in each case. As the number of sub-bands increase, the baud rate is reduced but the overall transmission speed remains the same.

Next, the candidate pulse shapes are shaped to form a Hilbert pair, meaning they occupy the same frequency range but are separated in phase by 90∘. The final pulse-shaping filters of the in-phase and quadrature parts are given by $p_l^I(n)$ and $p_l^Q(n)$, respectively, which are given by [14]:

$$
\begin{aligned}
p_l^I(n) &= g(n)\cos(2\pi f_l n) \\
p_l^Q(n) &= g(n)\sin(2\pi f_l n)
\end{aligned}
\tag{4}
$$

where $g(n)$ is one of the two candidate pulse shapes, i.e. the square-root raised cosine (SRRC) or Xia pulse, and f_l is the carrier frequency of the lth sub-band, given by [14]:

$$
f_l = \frac{2l-1}{2m}BW
\tag{5}
$$

Finally, the transmitted signal $x(n)$ is given by [14]:

$$
x(n) = \sqrt{2}\sum_{l=1}^{m} X_l^I(n) * p_l^I(n) - X_l^Q(n) * p_l^Q(n)
\tag{6}
$$

where $X_l^I(n)$ and $X_l^Q(n)$ correspond respectively to the in-phase and quadrature components of the data symbol to be carried on the lth sub-band.

Following modulation, the data is framed and prepared for the DAC according to the JESD-204B standard. We have used a 16-bit DAC (i.e., AD9152) with a maximum sample rate of 2.25 GS/s that is connected to the ZCU102 via the mezzanine connector. Note, we select our sampling frequency f_s as 1.25 GS/s to match the analogue-to-digital (ADC) converter maximum sampling frequency.

Next, the converted data stream is amplified prior to intensity modulation of an 850 nm laser diode (Laser Components PV85G0.53FCA-0-0-01) at 1 mW via a bias-tee (Mini Circuits ZFBT-6GW+). The intensity modulated light signal is then collimated using a ThorLabs F240FC-850 lens prior to transmission over the free-space channel.

We utilise a fibre optic cable to guide the light from the laser to the entrance of the free-space atmospheric chamber. The light emitted is collimated and transmitted across the chamber. At the receiver, we capture the light via a lens into a separate fibre. This approach allows rapid and simple alignment of the free-space system which can also be a timely operation, and also enables maximum coupling efficiency. On the other hand, depending on the divergence angle of transmitter beam, there is limit on longest link distance before the optical beam size at the receiver exceeds the frontend aperture, hence exposing the link to geometric loss. Reducing the divergence angle avoids this issue, however, this introduces a requirement for increasingly large optical components, increasing the price, size and maximum link distance. However, larger optics at the transmitter will

escalate the effect of pointing errors due to smaller beam size since the side effect of beam pointing error is more pronounced on more collimated beams. On the other hand, having a larger receiver aperture will improve the resilience of the link towards pointing errors as the jittering beam will remain within the receiver active area. Apart from geometric loss and pointing error, the alignment of the system is also highly affected by the size of the optics. A narrow beam (i.e., a small footprint at the receiver) will make the alignment process a tedious job. Therefore, the middle ground, where the optimum transmitter divergence angle and receiver aperture size are adopted, as has been discussed extensively in previous work [10], [22].

We have utilised the world-leading indoor atmospheric chamber at Northumbria University to evaluate the FSO link performance under different conditions [10] (a representative photo in Fig. 4).
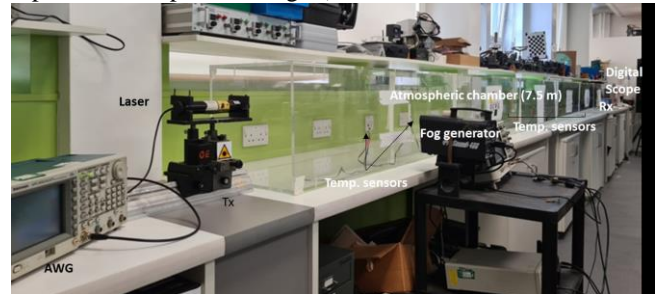

Fig. 4 Representative photograph of the atmospheric chamber under use in this test. Alternate equipment was used in this paper as described in the text.

The chamber is configured to emulate a fog environment and we have used neutral density filters to control the received power P_r to maintain consistency throughout the test and measurement. Since the FSO channel has been extensively studied and reported in the literature extensively [10], we do not discuss it in detail here. However, it should be noted that we only investigate the impact of fog on the performance of the FSO link and have not considered others channel conditions such as turbulence. Fog results in a reduction of visibility V due to aerosol scattering, which can be modelled with a coefficient β_α as follows [23]:

$$
\beta_\alpha(\lambda) = \frac{3.91}{V}\left(\frac{\lambda}{550\ \text{nm}}\right)^{-q}
\tag{7}
$$

where λ is the wavelength and q is the size distribution of the scattering particles given by the Kim model in [24], which has been used as a valid approach to of modelling in FSO for many years.

The receiver consists of a focusing lens (ThorLabs F240FC-850) followed by a photodiode (ThorLabs DET025AFC), a transimpedance amplifier (Texas Instruments OPA855DSGEVM), and a limiting amplifier (AD MAX3747), which feeds the ADC (AD9680, 14-bits with a maximum sample rate $f_{s\text{-max}}$ of 1.25 GS/s).

The most critical aspect of real-time system performance

is the clock recovery, which must be carried out properly in order to ensure that the data can be fully recovered. Here, we have employed the Schmidl & Cox method traditionally used with OFDM modulation, in which the first symbol in a frame is transmitted with known information. Considering that the free-space channel is static, flat in terms of its frequency response and its profile is only sensitive to the received power, we hypothesize that there should be little difference in system performance between a frame structure where one synchronisation frame is transmitted before continuous data, rather than re-syncing periodically as there is no new channel information to obtain, provided the link remains undisturbed.

After the data is de-framed, synchronisation is performed before the data is demodulated. In general, *m*-CAP signals are demodulated using time-reversed matched filters, a one-tap equaliser and hard threshold detection. The time-reversed matched filters are given as $f(n) = g(-n)$.

III. RESULTS

We evaluate the performance of the proposed *m*-CAP FSO system by analysis of the error vector magnitude (EVM) in this section. For each of our measurements we captured at least 107 symbols.

In Fig. 5, we illustrate the EVM performance of the link operating at 0.5 Gb/s, using both pulse shapes for all *m* and $\beta = 0.35$. Based on previous studies in band-limited optical wireless links [21], we anticipated that a higher order of *m* would improve the system performance, particularly in low power environments due to the lower sub-band baud rates. However, the results show the opposite trend is true; the systems that used the higher value of *m* actually demonstrate worse EVM performance in low visibilities (i.e. $P_r < -13$ dBm) and the single sub-band system has greater sensitivity. This is also true for all values of β tested. This is attributed to a relatively large null observed in the frequency response of the receiver electronics. The null is observed at approximately 210 MHz and the bandwidth of the *m*-CAP signal is 300 MHz. We believe that this null is the result of destructive interference caused by an impedance mismatch in our receiver. Therefore, for systems not AWGN limited, transmitting a 1-CAP signal would entail utilising the entire spectrum, which could then be easily corrupted due to the large null in the frequency response. This explains why the signal recovers to lower EVM levels when *m* is increased in higher received power environments. Similar results were obtained for the $k = 2$ and 6 systems, which are not shown here in the interest of conserving space. Note, in our previous work, we demonstrated that by dividing the *m*-CAP signal into increasingly small sub-bands, the channel begins to appear flat to each individual sub-band, regardless of the overall shape and we believe this is why the spectral null impacts the higher order subcarriers less [21].

We also observed that the SRRC consistently outperformed the Xia pulse, counter to previous reports [14]. While the performances are similar, the Xia pulse

consistently has a small sensitivity penalty. Since our electro-optic system is not band-limited and we are comfortably within the linear region of operation, we attribute this to the fact that the Xia pulse has a centre-offset peak. This offset is the source of the penalty since the optimal sampling point has a lower SNR than the SRRC due to the nature of the offset. Previous reports tested the Xia pulse in a highly bandlimited system that introduced significant non-linearity, hence the different outcome. Furthermore, there have been no real-time reports on the performance of the Xia pulse so far. Previous efforts have performed data capture via a real-time oscilloscope, meaning that the optimal sampling point can always be found, benefitting performance in a way that cannot be matched in this work.
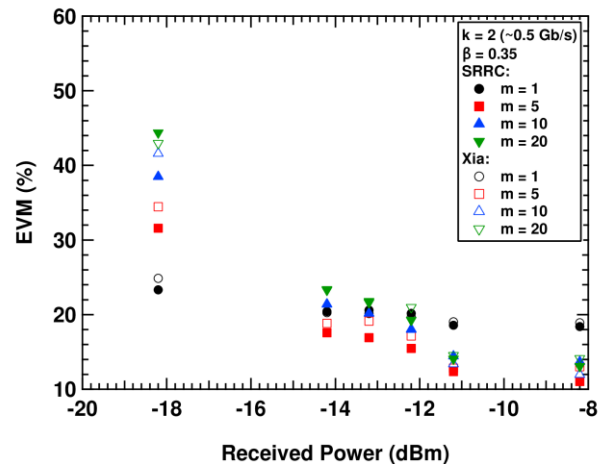

Fig. 5 EVM performance of the ~0.5 Gb/s illustrating the sub-band specific performance of the link for both filters under test.

In Fig. 6, we illustrate the comparative performance of the two pulse shaping filter candidates using *m* of 1 and 20 operating at ~1 Gb/s. The same observation as above occurs where the system with the higher number of sub-bands performs better at higher received power values and the single-band system operates better in lower received powers. We include two values of β to illustrate that the effect is independent from it. We also note that for $k = 6$, a similar trend is observed. We also note that there is little difference in performance between the Xia and SRRC in the most part.
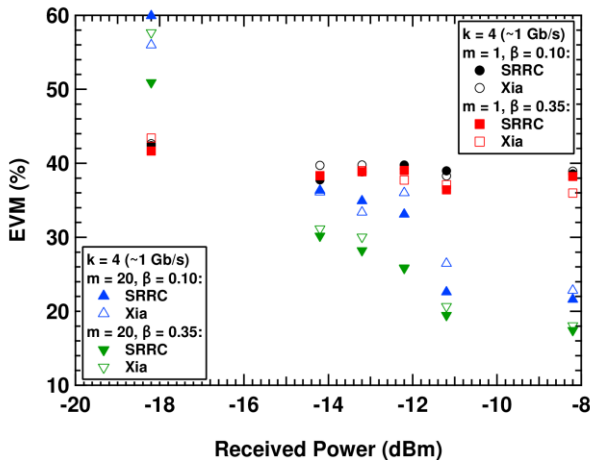
Fig. 6 EVM performance of the ~1 Gb/s link for varying numbers of sub-bands and roll-off factors.

Next, in Fig. 7 we compare the performance of the ~0.5 and ~1 Gb/s systems for a fixed value of $\beta = 0.35$. Clearly, both systems follow similar trends judging by their EVM profile trends. In both cases, when the system is noise limited the performance of the 1-CAP system is superior and vice-versa in high performance environment. Interestingly, the increase in performance for the ~1 Gb/s system in higher received powers (i.e. -8 dBm) is substantially larger than it is for the ~0.5 Gb/s system. For the former, the EVM improves from ~40 to ~18%, while for the latter, the improvement is from ~18 to ~14%. We attribute this to a combination of the performance gain introduced with higher sub-bands mentioned previously in the discussion of Fig. 5 and the fact that increasing the received power alleviates the far greater SNR penalty imposed on the system for 16-QAM in comparison to 4-QAM. Similar trends are also observed when $k = 6$ which are not shown here. The performance of this system (~1.5 Gb/s) is an approximate EVM value of ~20% for $m = 10$ and 20 at a received power of -8.2 dBm.
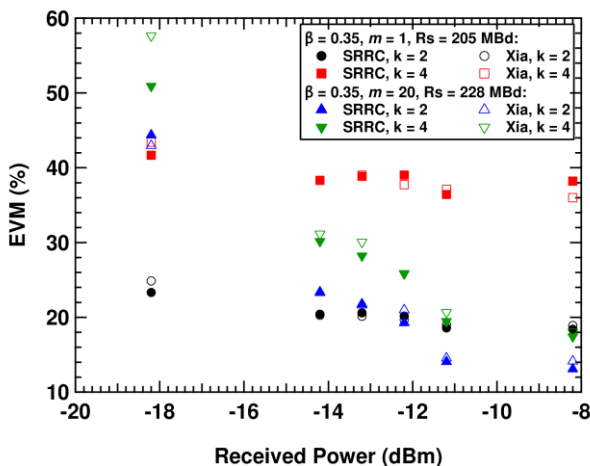

Fig. 7 EVM performance of the ~0.5 and ~1 Gb/s FSO links with a roll-off factor of 0.35. The performance gain for the ~1 Gb/s system at high received power outperforms that of the ~0.5 Gb/s equivalent.

IV. CONCLUSION

In this paper we have compared the EVM performance of a real-time FSO platform that utilises m-CAP modulation. Using an indoor atmospheric chamber, we tested the SRRC and Xia pulses in terms of their EVM performance at data rates of ~0.5, ~1 and ~1.5 Gb/s. We show data rates exceeding 1 Gb/s can be obtained for both pulse shapes and that they can be supported using many sub-bands.

REFERENCES

[1] M. P. J. Lavery *et al.*, "Tackling Africa's digital divide," *Nature Photonics 2018 12:5*, vol. 12, no. 5, pp. 249–252, Apr. 2018, doi: 10.1038/s41566-018-0162-z.

[2] A. K. Majumdar, "Technology Developments, Research Challenges, and Advances for FSO Communication for Space/Aerial/Terrestrial/Underwater (SATU) Links," *Laser Communication with Constellation Satellites, UAVs, HAPs and Balloons*, pp. 129–158, 2022, doi: 10.1007/978-3-031-03972-0_5.

[3] A. Trichili, M. A. Cox, M. A. Cox, B. S. Ooi, and M.-S. Alouini, "Roadmap to free space optics," *JOSA B, Vol. 37, Issue 11, pp. A184-A201*, vol. 37, no. 11, pp. A184–A201, Nov. 2020, doi: 10.1364/JOSAB.399168.

[4] W. Song *et al.*, "Influence of fog on the signal to interference plus noise ratio of the imaging laser radar using a 16-element APD array," *Optics Express, Vol. 26, Issue 17, pp. 22030-22045*, vol. 26, no. 17, pp. 22030–22045, Aug. 2018, doi: 10.1364/OE.26.022030.

[5] M. Komanec, W. O. Popoola, Z. Ghassemlooy, S. Zvanovec, J. Libich, and P. Pesek, "Experimental verification of an all-optical dual-hop 10 Gbit/s free-space optics link under turbulence regimes," *Optics Letters, Vol. 40, Issue 3, pp. 391-394*, vol. 40, no. 3, pp. 391–394, Feb. 2015, doi: 10.1364/OL.40.000391.

[6] M. Singh and J. Malhotra, "Performance comparison of M-QAM and DQPSK modulation schemes in a 2 × 20 Gbit/s–40 GHz hybrid MDM–OFDM-based radio over FSO transmission system," *Photonic Network Communications*, vol. 38, no. 3, pp. 378–389, Dec. 2019, doi: 10.1007/S11107-019-00861-Z/METRICS.

[7] K. Anbarasi, C. Hemanth, and R. G. Sangeetha, "Block error rate performance analysis of RS coded M-QAM modulated coherent OFDM-FSO system," *Opt Quantum Electron*, vol. 55, no. 1, pp. 1–15, Jan. 2023, doi: 10.1007/S11082-022-04328-W/METRICS.

[8] W. O. Popoola and Z. Ghassemlooy, "BPSK Subcarrier Intensity Modulated Free-Space Optical Communications in Atmospheric Turbulence," *Journal of Lightwave Technology, Vol. 27, Issue 8, pp. 967-973*, vol. 27, no. 8, pp. 967–973, Apr. 2009,

Accessed: Jan. 29, 2023. [Online]. Available: https://opg.optica.org/abstract.cfm?uri=jlt-27-8-967

[9] M. Capelle, M. J. Huguet, N. Jozefowiez, and X. Olive, "Optimizing ground station networks for free space optical communications: Maximizing the data transfer," *Networks*, vol. 73, no. 2, pp. 234–253, Mar. 2019, doi: 10.1002/NET.21859.

[10] Z. Htay, Z. Ghassemlooy, M. M. Abadi, A. Burton, N. Mohan, and S. Zvanovec, "Performance Analysis and Software-Defined Implementation of Real-Time MIMO FSO with Adaptive Switching in GNU Radio Platform," *IEEE Access*, vol. 9, pp. 92168–92177, 2021, doi: 10.1109/ACCESS.2021.3092968.

[11] J. Chen, J. Shi, J. Hu, C. Shen, and N. Chi, "DC-balanced even-dimensional CAP modulation for visible light communication," *Journal of Lightwave Technology*, vol. 40, no. 15, pp. 5041–5051, 2022.

[12] J. Chen et al., "Neural network detection for bandwidth-limited non-orthogonal multiband CAP UVLC system," *IEEE Photonics J*, vol. 14, no. 2, pp. 1–9, 2022.

[13] X.-G. Xia, "A family of pulse-shaping filters with ISI-free matched and unmatched filter properties," *IEEE Transactions on Communications*, vol. 45, no. 10, pp. 1157–1158, 1997.

[14] P. A. Haigh, P. Chvojka, S. Zvánovec, Z. Ghassemlooy, and I. Darwazeh, "Analysis of Nyquist Pulse Shapes for Carrierless Amplitude and Phase Modulation in Visible Light Communications," *Journal of Lightwave Technology*, vol. 36, no. 20, pp. 5023–5029, Oct. 2018, doi: 10.1109/JLT.2018.2869022.

[15] A. M. Shah et al., "Characterization of RF signal transmission using FSO links considering atmospheric effects," in *Free-Space Laser Communication Technologies XX*, 2008, pp. 112–121.

[16] C. Ben Naila, A. Bekkali, K. Wakamori, and M. Matsumoto, "Performance analysis of CDMA-based wireless services transmission over a turbulent RF-on-FSO channel," *Journal of Optical Communications and Networking*, vol. 3, no. 5, pp. 475–486, 2011.

[17] P. T. Dat et al., "Studies on characterizing the transmission of RF signals over a turbulent FSO link," *Opt Express*, vol. 17, no. 10, pp. 7731–7743, 2009.

[18] T. Wang, S. Bin Ali Reza, F. Buldt, P. Bassène, and M. N'Gom, "Structured light signal transmission through clouds," *J Appl Phys*, vol. 133, no. 4, 2023.

[19] N. Cvijetic, D. Qian, J. Yu, Y.-K. Huang, and T. Wang, "Polarization-multiplexed optical wireless transmission with coherent detection," *Journal of Lightwave Technology*, vol. 28, no. 8, pp. 1218–1227, 2010.

[20] D. S. Kim, "Hybrid Free-Space and Radio Frequency Switching," 2008.

[21] P. A. Haigh et al., "A Multi-CAP Visible-Light Communications System with 4.85-b/s/Hz Spectral Efficiency," *IEEE Journal on Selected Areas in Communications*, vol. 33, no. 9, pp. 1771–1779, Sep. 2015, doi: 10.1109/JSAC.2015.2433053.

[22] M. M. Abadi, Z. Ghassemlooy, S. Zvanovec, M. R. Bhatnagar, and Y. Wu, "Hard switching in hybrid FSO/RF link: Investigating data rate and link availability," *2017 IEEE International Conference on Communications Workshops, ICC Workshops 2017*, pp. 463–468, Jun. 2017, doi: 10.1109/ICCW.2017.7962701.

[23] M. K. El-Nayal, M. M. Aly, H. A. Fayed, and R. A. AbdelRassoul, "Adaptive free space optic system based on visibility detector to overcome atmospheric attenuation," *Results Phys*, vol. 14, p. 102392, Sep. 2019, doi: 10.1016/J.RINP.2019.102392.

[24] I. I. Kim, B. McArthur, and E. J. Korevaar, "Comparison of laser beam propagation at 785 nm and 1550 nm in fog and haze for optical wireless communications," *https://doi.org/10.1117/12.417512*, vol. 4214, pp. 26–37, Feb. 2001, doi: 10.1117/12.417512.

Paul Anthony Haigh received the BEng(H) and Ph.D. degrees from Northumbria University, Newcastle upon Tyne, U.K., in 2010 and 2014, respectively. From 2011 to 2012, he was the European Organisation for Nuclear Research (CERN) with the prestigious Marie Curie Fellowship working on optical fibre links for high energy physics experiments. During his Ph.D., he pioneered the topic of organic visible light communications. From 2014 to 2016, he was a Senior Research Associate with the High-Performance Networks Group, University of Bristol, working on reconfigurable agile network interfaces. From 2016 to 2019, he was a Senior Research Associate at University College London working on high-speed polymer visible light communications systems, with particular focus on modulation, digital signal processing and healthcare applications. In 2019, he was appointed as a Lecturer in communications and signal processing at the School of Engineering, Newcastle University. From 2021-2022 he was a Development Engineer at Toshiba Europe at the Cambridge Research Laboratory, UK working on quantum information systems. Since 2022 he is a Principal Systems Engineer at Nubis Communications, NJ, USA.

MOJTABA MANSOUR ABADI received the B.Sc. degree in electrical engineering from Islamic Azad University, Fasa, Iran, in 2005, the M.Sc. degree in electromagnetic fields and waves from the K. N. Toosi University of Technology, Tehran, Iran, in 2008, and the Ph.D. degree in optical communication from the Optical Communications Research Group (OCRG), Northumbria University, Newcastle upon Tyne, U.K., in 2016. He is currently a Lecturer with the Department of Mathematics, Physics, and Electrical Engineering, Northumbria university. His main research interests

include optical devices, optics, electronics and optics prototyping, terrestrial optical communications, and space optical communications.

ZABIH GHASSEMLOOY received the B.Sc. degree (Hons.) in electrical engineering from Manchester Metropolitan University, in 1981, and the M.Sc. and Ph.D. degrees from The University of Manchester, U.K., in 1984 and 1987, respectively. From 1987 to 1988, he was a Postdoctoral Research Fellow with the City, University of London, U.K. From 1988 to 2004, he was with Sheffield Hallam University, U.K. From 2004 to 2014, he was an Associate Dean (Research) with the Faculty of Engineering and Environment, Northumbria University, U.K., where he is currently the Head of Optical Communications Research Group. Since 2016, he has been a Research Fellow with the Chinese Academy of Sciences, where he has been a Distinguished Professor, since 2015. He has published over 980 papers (more than 425 journals and eight books) with several best paper awards, given more than 100 keynote/invited talks, and supervised 12 research fellows and 75 Ph.D. students. His research interests include optical wireless communications, free space optics, visible light communications, and hybrid RF and optical wireless communications. He is a fellow of SOA and IET. He was the Vice-Chair of EU Cost Action IC1101 (2011–2016). He is the Vice-Chair of the EU COST Action CA19111 NEWFOCUS (European Network on Future Generation Optical Wireless Communication Technologies; 2020–2024). He is the Chief Editor of the British Journal of Applied Science and Technology and the International Journal of Optics and Applications, an associate editor of a number of international journals, and the co-guest editor of a number of OWC special issues. He has been the Vice-Chair of the OSA Technical Group of Optics in Digital Systems, since 2018. He has been the Chair of the IEEE Student Branch, Northumbria University, Newcastle upon Tyne, since 2019. From 2004 to 2006, he was the IEEE U.K./IR Communications Chapter Secretary, the Vice-Chairman (2006–2008), the Chairman (2008–2011), and the Chairman of the IET Northumbria Network (2011–2015).

Quang Nguyen-The was born in Bac Ninh, Viet Nam, in 1978. He received B.E. degree from National Defense Academy, Japan in 2004, M.E. degree in 2009 and the Ph.D degree in 2012 from the University of Electro-Communications, Tokyo, Japan. He was as a postdoctoral fellow researcher in Department of Communication Engineering and Informatics, the University of Electro-Communications, Tokyo, Japan from 2012 to 2014. Mr. Quang is a Member of Institute of Electronics, Information and Communication Engineers of Japan. He was the recipient of the Young Scientist Award in the 15th OptoElectronics and Communications Conference (OECC 2010) presented by the IEEE Photonics Society Japan Chapter. His research interest is in all-optical signal processing for WDM and OTDM systems, free-space optical communication system. He is currently an Associate Professor at Le Quy Don Technical University, Hanoi, Vietnam.
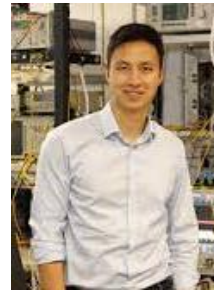
Son Thai Le attended Hanoi University of Science and Technology from 2006 to 2007. From 2007 to 2012, they attended Southern Federal University (former Rostov State University) and received a Bachelor of Engineering (B.Eng.) in Electrical, Electronics and Communications Engineering. Son then attended Aston University from 2013 to 2016, where they earned a Doctor of Philosophy (Ph.D.) in Laser and Optical Engineering. Son started as a Research Assistant at the Laboratory of Radio Transmitter Devices at SFedU, where they proposed a novel and effective method to control the chaotic regime of semiconductor laser subjected to external injection, proposed a novel analytical method for analysing the nonlinear dynamics of semiconductor laser subjected to external injection, and proposed and demonstrated a novel self-heterodyne detection method for amplitude-shift-keying optical signals. From 2013 to 2016, they worked at Aston University as a Postdoctoral Research Fellow and PhD student. During this time, he demonstrated the world first transmission based on the modulation of continuous part of the nonlinear signal spectrum, achieving a record distance reach of 7344km, and demonstrated two novel flexible nonlinear compensation techniques for CO-OFDM, which can be applied effectively in WDM transmissions and optical links with ROADM. Son also invented a novel quasi-pilot-aided phase noise compensation technique for CO-OFDM systems, which effectively reduces the pilot subcarrier overhead by a factor of 2. Since 2016, he has been a Member of Technical Staff and Research Engineer at Nokia Bell Labs, and since 2022 he has been a Principal Systems Engineer at Nubis Communications.
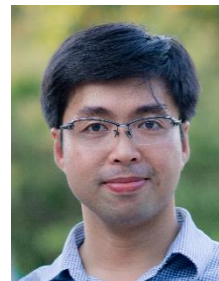
Nguyen Tan Hung was born in Danang, Viet Nam, in 1980. He received the B.E. degree from The University of Danang-University of Science and Technology, Da Nang, Vietnam, in 2003, and the M.E. and Ph.D. degrees from the University of Electro-Communications, Tokyo, Japan, in 2009 and 2012, respectively. From 2012 to 2016, he was a Researcher with the National Institute of Advanced Industrial Science and Technology, Tsukuba, Japan, where he worked on ultrafast and spectrally efficient all-optical network technologies, and development of an all-optical wavelength converter. In 2016, he joined The University of Danang, Danang, Vietnam, where he is currently an Associate Professor and the Vice-Director of The University of Danang-Advanced Institute of Science and Technology. His research interests include optical communications and networking, all-optical signal processing and photonic integrated circuits.